RESEARCH ARTICLE

What's Special About Task in Dystonia? A Voxel-Based Morphometry and Diffusion Weighted Imaging Study

Ritesh A. Ramdhani, MD,[1] Veena Kumar,[1] Miodrag Velickovic, MD,[1] Steven J. Frucht, MD,[1] Michele Tagliati, MD,[3] and Kristina Simonyan, MD, PhD[1,2]*

[1]*Department of Neurology, Icahn School of Medicine at Mount Sinai, New York, New York, USA*
[2]*Department of Otolaryngology, Icahn School of Medicine at Mount Sinai, New York, New York, USA*
[3]*Department of Neurology, Cedars-Sinai Medical Center, Los Angeles, California, USA*

ABSTRACT: Numerous brain imaging studies have demonstrated structural changes in the basal ganglia, thalamus, sensorimotor cortex, and cerebellum across different forms of primary dystonia. However, our understanding of brain abnormalities contributing to the clinically well-described phenomenon of task specificity in dystonia remained limited. We used high-resolution magnetic resonance imaging (MRI) with voxel-based morphometry and diffusion weighted imaging with tract-based spatial statistics of fractional anisotropy to examine gray and white matter organization in two task-specific dystonia forms, writer's cramp and laryngeal dystonia, and two non–task-specific dystonia forms, cervical dystonia and blepharospasm. A direct comparison between both dystonia forms indicated that characteristic gray matter volumetric changes in task-specific dystonia involve the brain regions responsible for sensorimotor control during writing and speaking, such as primary somatosensory cortex, middle frontal gyrus, superior/inferior temporal gyrus, middle/posterior cingulate cortex, and occipital cortex as well as the striatum and cerebellum (lobules VI-VIIa). These gray matter changes were accompanied by white matter abnormalities in the premotor cortex, middle/inferior frontal gyrus, genu of the corpus callosum, anterior limb/genu of the internal capsule, and putamen. Conversely, gray matter volumetric changes in the non–task-specific group were limited to the left cerebellum (lobule VIIa) only, whereas white matter alterations were found to underlie the primary sensorimotor cortex, inferior parietal lobule, and middle cingulate gyrus. Distinct microstructural patterns in task-specific and non–task-specific dystonias may represent neuroimaging markers and provide evidence that these two dystonia subclasses likely follow divergent pathophysiological mechanisms precipitated by different triggers. © 2014 International Parkinson and Movement Disorder Society

Key Words: brain imaging; task specificity; focal dystonia

Task specificity in primary focal dystonia is a clinically well-described but poorly understood phenomenon. Although brain abnormalities in the basal ganglia, sensorimotor cortex, and cerebellum are identified across different forms of dystonia,[1-3] specific alterations in these brain regions that may differentiate between task-specific (TSD) and non–task-specific (NTSD) dystonias are unknown.

Generally, in patients with task-specific focal hand dystonia, writer's cramp, changes in gray matter volume (GMV) are reported in the hand region of the sensorimotor cortex, putamen, thalamus, and cerebellum,[4-7] with white matter integrity changes in the posterior limb of the internal capsule and adjacent structures.[8] In another form of TSD, laryngeal dystonia or spasmodic dysphonia, we recently identified decreased white matter integrity in the genu of the internal capsule as well as increased GMV in the laryngeal sensorimotor cortex, inferior frontal, superior/middle temporal, and supramarginal gyri,

*Correspondence to: Kristina Simonyan, MD, PhD, Department of Neurology, One Gustave L. Levy Place, Box 1137, Icahn School of Medicine at Mount Sinai,New York, NY 10029, E-mail: kristina.simonyan@mssm.edu

Funding agencies: This study was supported by Bachmann-Strauss Dystonia and Parkinson Foundation and NIDCD/NIH (R01DC011805) to K. Simonyan, the National Center for Advancing Translational Sciences, NIH (UL1TR000067) to Mount Sinai Clinical Research Center.

Relevant conflicts of interest/financial disclosures: Nothing to report. Full financial disclosures and author roles may be found in the online version of this article.

Received: 20 August 2013; **Revised:** 6 May 2014; **Accepted:** 7 May 2014

Published online 12 June 2014 in Wiley Online Library (wileyonlinelibrary.com). DOI: 10.1002/mds.25934

putamen, and cerebellum.[9,10] In NTSD forms, such as cervical dystonia, increased GMV has been found in the motor cortex, globus pallidus, and cerebellum,[11] whereas white matter abnormalities were identified in the genu and body of the corpus callosum and the basal ganglia.[12] In addition, a recent study found reduced basal ganglia GMV in the unaffected familial relatives of patients with cervical dystonia.[13] Studies in patients with non–task-specific blepharospasm reported GMV increases in the putamen[14,15] and reductions in the inferior parietal lobule[15] as well as reduced left corticobulbar tract volume and connectivity.[16] Although, collectively, these studies are highlighting the basal ganglia, sensorimotor cortex, and cerebellum as the main brain regions altered across different forms of dystonia, the lack of knowledge about the disorder-specific changes in patients with TSD and NTSD limits our understanding of the pathophysiology of these disorders and, consequently, our ability to identify their neuroimaging biomarkers.

The aim of this comparative study was to examine gray and white matter alterations in patients with two forms of TSD (writer's cramp and laryngeal dystonia) and two forms of NTSD (cervical dystonia and blepharospasm), using high-resolution magnetic resonance imaging (MRI) with voxel-based morphometry (VBM) and diffusion weighted imaging with tract-based spatial statistics. We hypothesized that abnormalities in TSD would affect the focal segments of brain circuits, which are critical for planning and execution of highly learned tasks in humans, such as writing and speaking, respectively, whereas brain changes in NTSD patients would be more uniform and symmetrically involving both hemispheres. We also expected that abnormalities in the basal ganglia and cerebellum would represent common changes across different types of dystonia, both with and without task specificity.

Materials and Methods

Participants

We recruited 45 patients with focal dystonias, who had been diagnosed with TSD (12 writer's cramp and 12 laryngeal dystonia) or NTSD (11 cervical dystonia and 10 blepharospasm) as well as 24 healthy controls. The NTSD patients did not show preferential specificity to different tasks at the time of the recruitment, thus validating their dystonia type as NTSD. No statistical differences were seen in age and sex between either the patient groups or each patient group and controls (all $P > 0.15$) (Table 1). The participants had no neurological (except focal dystonia in the patient group), psychiatric, or laryngeal problems based on history or physical and neurological examinations. All participants were right-handed and fully symptomatic at the time of study participation. Those who received botulinum toxin treatment were recruited at the end of their treatment cycle, at least 3 months postinjection. The mean duration of the disorder was 16.5 ± 12.9 years in writer's cramp, 10.2 ± 6.3 years in laryngeal dystonia, 12.3 ± 8.9 years in cervical dystonia, and 7.3 ± 4.5 years in blepharospasm. Duration of the disorder was not significantly different between the patient groups (all $P > 0.05$). Clinical neuroradiological evaluation of MRI in all subjects showed normal brain structure without any gross abnormalities.

All participants provided written informed consent, which was approved by the Institutional Review Board of the Icahn School of Medicine at Mount Sinai.

Image Acquisition

High-resolution T1-weighted images were acquired on a 3T Phillips scanner equipped with an eight-channel receive-only coil using a three-dimensional magnetization prepared rapid acquisition gradient echo (MPRAGE) sequence with TI = 450 ms; TE = 2.9 ms; flip angle = 10 degrees; FOV = 240 mm; matrix = 256 × 256 mm; 172 contiguous axial slices; slice thickness = 0.9 mm. Diffusion-weighted images were acquired using a single-shot spin-echo echo-planar imaging sequence with paired gradient pulses positioned 180° around the refocusing pulse for diffusion weighting (TR = 13 000 ms, FOV = 240 mm; matrix = 96 × 96 mm zero-filled to 256 × 256 mm; 54 contiguous axial slices with slice thickness of 2.4 mm). Diffusion was measured along 33 noncollinear directions with a b-factor of 1,000 s/mm^2. One reference image was acquired with no diffusion gradients applied (b0 scan).

Voxel Based Morphometry

Using SPM8 software with VBM8 toolbox, raw images were bias corrected for MRI inhomogeneities and noise, tissue-classified, co-registered, and normalized to a standard Montreal Neurological Institute (MNI) space using DARTEL (diffeomorphic anatomical registration using exponentiated lie algebra).[17] Tissue probability maps were warped onto the image nonlinearly, allowing for tissue segmentation. Jacobian determinants were used to modulate GMV through multiplication of nonlinear components derived during normalization to preserve tissue volume after warping. The spatially normalized images were smoothed with an isotropic 8-mm Gaussian kernel.

To examine structural brain differences in relation to clinical phenomenology (TSD vs. NTSD) and estimate the main effect, one-way analysis of variance (ANOVA) with one factor (GMV) and three levels (controls, TSD, NTSD) was carried out at an family-wise error (FWE)-corrected $P \leq 0.05$. The FWE rate was determined using Monte Carlo simulations,[18,19]

TABLE 1. Demographic and clinical data

	Cervical dystonia	Blepharospasm	Laryngeal dystonia	Writer's cramp	Controls	*P*-value[a]
Number of subjects	11	10	12	12	24	N/A
Age (mean), [range]	57.28[29-77]	59.2[45-69]	54.75[44-66]	52.75[21-72]	52.13[38-71]	All between-patient $P > 0.16$; all patient–control $P > 0.05$
Sex (female/male)	7/4	9/1	8/4	6/5	12/12	All between-patient $P > 0.15$; all patient–control $P > 0.05$
Disease duration (y) mean ± standard deviation	12.3 ± 8.9	7.3 ± 4.5	10.2 ± 6.3	16.5 ± 12.9	N/A	All between-patient $P > 0.05$

[a]Comparisons were made between each patient group and controls as well as between the patient groups using two-sample *t*-test or Fisher's exact test, wherever appropriate. N/A, not applicable.

which resulted in identification of a minimum cluster size of 528 mm^3 at a voxelwise threshold of 0.001.

The follow-up post hoc two-sample *t* tests with age, sex, total intracranial volume, and duration of the disorder as nuisance covariates were performed to determine statistical differences of GMV changes between TSD/NTSD and controls as well as between TSD and NTSD directly. The severity of disorder was not included as a covariate because these data were not available in all patients. The overall statistical significance for between-group comparisons was set at a corrected $P \leq 0.016$ to account for multiple group comparisons. In addition, voxelwise correction for multiple comparisons was achieved by applying FWE correction to each comparison separately, using Monte Carlo simulations (minimum cluster size, 150 mm^3; voxelwise threshold, 0.01).

Diffusion Weighted Imaging

Using FSL software, images were brain extracted and corrected for movement artifacts and eddy current distortions. The fractional anisotropy (FA) maps were calculated and registered to a standard MNI space using nonlinear registration. Following the creation of a mean FA skeleton and registration of each individual FA map to the skeleton, whole-brain voxelwise statistical analyses were conducted using tract-based spatial statistics (TBSS).[20] One-way ANOVA with one factor (white matter skeleton) and three levels (controls, TSD, NTSD) was used to estimate the main effect at an FWE-corrected $P \leq 0.05$ (Monte Carlo simulations: voxelwise threshold, 0.001; minimum cluster size, 50 mm^3). The follow-up post hoc two-sample *t* tests with age, sex, and disorder duration examined differences in TSD/NTSD versus controls and TSD versus NTSD at a threshold-free cluster enhancement (TFCE)-corrected $P \leq 0.016$.[21]

In addition, we examined the statistical dependence of VBM/TBSS measures with disorder duration in TSD and NTSD using voxelwise Spearman's rank correlation coefficients at an FWE-corrected $P \leq 0.05$ (voxelwise threshold 0.001, minimum cluster size 18 mm^3).

Results

Voxel-Based Morphometry

Initial ANOVA between all groups found a significant main effect of GMV changes in the left anterior dorsal putamen, caudate nucleus, and ventral striatum (FWE-corrected $P \leq 0.05$). (Fig. 1A, Table 2).

Compared with healthy controls, NTSD showed increased GMV in the left primary sensorimotor cortex, middle temporal gyrus, thalamus, and bilateral cerebellum (lobule VIIa), whereas reduced GMV was found in the right middle frontal gyrus, inferior temporal gyrus, and occipital cortex as well as anterior dorsal putamen and ventral striatum bilaterally at a corrected $P \leq 0.016$ (Fig. 1B, Table 2). The TSD patients, compared with controls, demonstrated increased GMV in the left premotor cortex, inferior parietal lobule, cuneus, cerebellum (lobules VI and VIIa); right primary sensorimotor cortex, superior temporal gyrus, supramarginal gyrus; bilateral operculum/insula, and middle/inferior temporal gyrus at a corrected $P \leq 0.016$ (Fig. 1C, Table 2).

A direct comparison of TSD with NTSD showed GMV changes in the bilateral middle frontal gyrus, middle/posterior cingulate cortex, inferior temporal gyrus, anterior dorsal putamen and caudate nucleus, ventral striatum, cerebellum (lobules VI-VIIa); right primary somatosensory cortex, superior temporal gyrus, and occipital cortex in TSD. Gray matter differences in the left cerebellum (lobule VIIa) were specific to NTSD (Fig. 1D, Table 2).

The GMV in the right premotor cortex was negatively correlated with TSD duration ($r_s = -0.69$) (Fig. 1E). No statistically significant relationships were found between NTSD duration and GMV at an FWE-corrected $P \leq 0.05$.

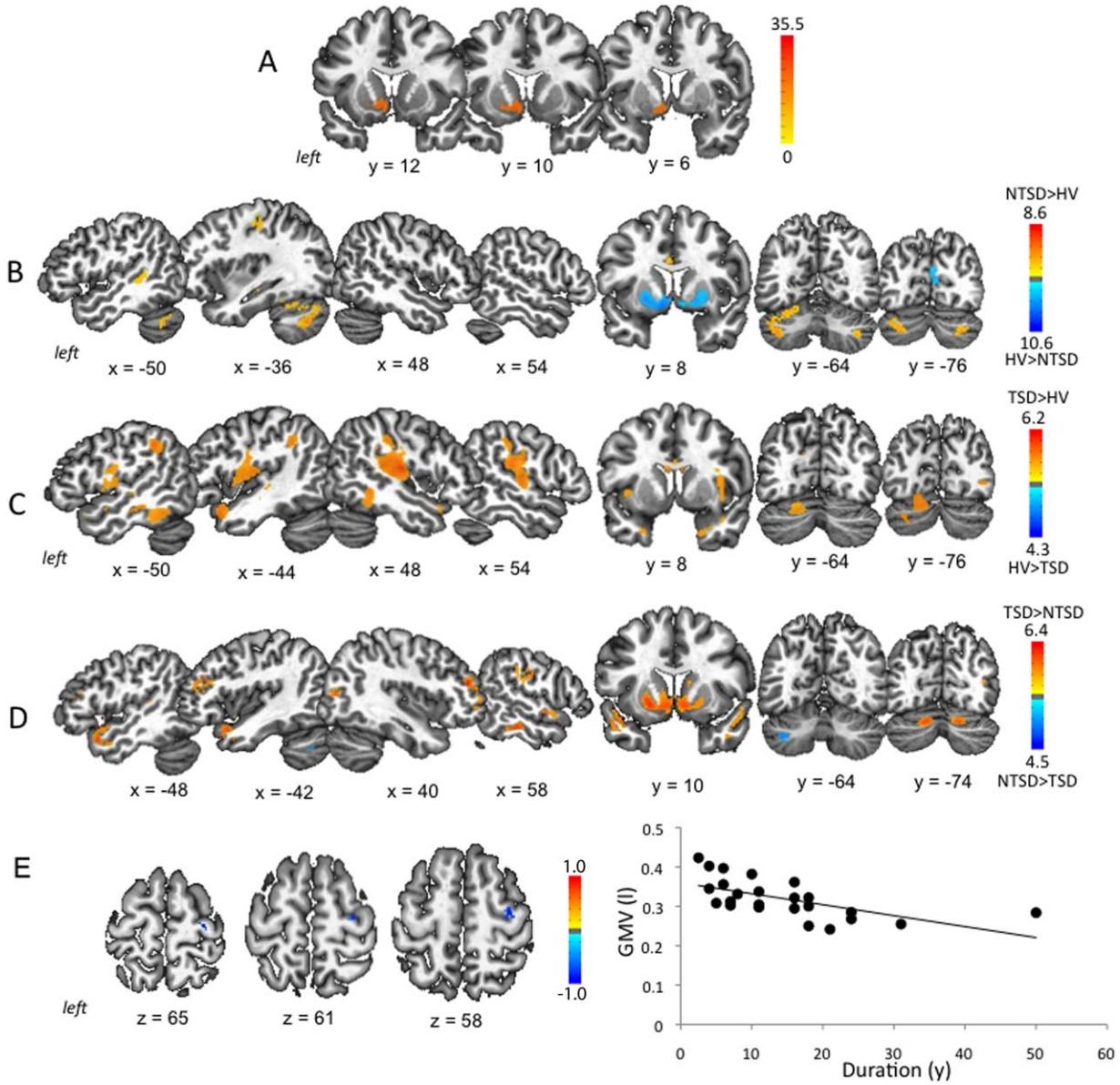

FIG. 1. Gray matter volumetric abnormalities in TSD and NTSD. (**A**) Results of initial analysis of variance (ANOVA) comparing gray matter volume (GMV) between TSD, NTSD, and healthy controls. (**B**) GMV differences between NTSD patients and healthy controls. (**C**) GMV differences between TSD patients and healthy controls. (**D**) Direct comparison of GMV differences between TSD and NTSD groups. (**E**) Significant inverse correlation between GMV (in liters) in the right premotor cortex and disorder duration (in years) in the TSD group. Brain abnormalities are shown on a series of axial, sagittal, and coronal sections in the standard MNI space. The corresponding coordinates of peak changes are given in Table 1. The color bars represent *F* score (**A**), *t* scores (**B, C, D**) and r_s score (**E**), respectively. TSD, task-specific dystonia; NTSD, non–task-specific dystonia.

Diffusion Weighted Imaging

Analysis of variance showed a significant main effect for between-group differences in the white matter underlying the bilateral middle frontal gyrus, primary sensorimotor cortices, occipital cortex, genu, and splenium of the corpus callosum, thalamus, midbrain/pons, cerebellum (lobules VI/VIIa), as well as the left operculum/insula, inferior parietal lobule/supramarginal gyrus, and middle/inferior temporal gyrus at an FWE-corrected $P \leq 0.05$ (Fig. 2A, Table 3).

Whole-brain analysis between NTSD and controls showed reduced FA in the genu and body of the corpus callosum, anterior limb/genu of the internal capsule, and in the white matter skeleton underlying the bilateral middle/inferior gyrus, right primary sensorimotor cortex, and inferior temporal gyrus at a corrected $P \leq 0.016$ (Fig. 2B, Table 3). In addition, NTSD exhibited increased FA in the splenium of the corpus callosum, bilateral cingulate gyrus, occipital cortex, midbrain/pons, cerebellum (lobule VIIa), and right ventral thalamus.

White matter changes were more localized in TSD compared with controls and included sparse FA reductions in the bilateral middle frontal gyrus, right anterior limb/genu of the internal capsule, and the left

TABLE 2. Gray matter changes between task-specific dystonia (TSD), non–task-specific dystonia (NTSD), and controls

		Brain region	*F-score*	*x,y,z*
Initial ANOVA	Left	Striatum	14.37	−3, 10, −14
GMV changes in NTSD/TSD vs. controls				
		Brain region	*T-score*	*x,y,z*
NTSD vs. Controls	Left	Primary sensorimotor cortex	3.82	−33, −27, 48
	Left	Middle temporal gyrus	3.06	−54, −41, 3
	Left	Thalamus	4.02	−9, −26, 12
	Left	Cerebellum (lobule VIIa)	5.58	−36, −69, −44
	Right	Cerebellum (lobule VIIa)	5.32	34, −71, −45
	Right	Middle frontal gyrus	−4.88	39, 54, −5
	Right	Inferior temporal gyrus	−4.71	60, −33, −23
	Right	Occipital cortex	−4.20	4, −78, 10
	Right	Striatum	−6.72	21, 12, −7
	Left	Striatum	−5.26	−21, 10, −6
TSD vs. Controls	Left	Premotor cortex	3.26	−36, −14, 60
	Left	Inferior parietal lobule	2.77	−51, −50, 38
	Left	Cuneus	4.32	−18, −54, 27
	Left	Cerebellum (lobules VI and VIIa)	3.79	−18, −80, −24
	Right	Primary sensorimotor Cortex	2.86	45, −24, 32
	Right	Superior temporal gyrus	4.53	48, −17, 10
	Right	Supramarginal gyrus	3.27	49, −27, 36
	Left	Operculum/insula	3.44	−45, −9, 9
	Right	Operculum/insula	3.11	40, 5, 2
	Left	Middle temporal gyrus	3.55	−50, −33, −14
	Left	Inferior temporal gyrus	4.13	−47, −45, 37
	Right	Middle/inferior temporal gyrus	3.01	49, −47, −12
GMV changes in TSD vs. NTSD			*T−score*	*x,y,z*
TSD > NTSD	Left	Middle/inferior frontal gyrus	4.25	−44, 31, 20
	Right	Middle frontal gyrus	6.42	39, 44, 16
	Left	Middle/posterior cingulate cortex	3.30	−1, −30, 32
	Right	Middle/posterior cingulate cortex	4.57	4, −35, 36
	Left	Inferior temporal gyrus	4.71	−57, −38, −19
	Right	Inferior temporal gyrus	5.34	57, −29, −21
	Left	Striatum	5.24	−21, 10, −6
	Right	Striatum	3.86	23, 13, −5
	Left	Cerebellum (lobule VI−VIIa)	4.85	−18, −71, −30
	Right	Cerebellum (lobule VI−VIIa)	4.39	16, −74, −29
	Right	Primary somatosensory cortex	3.94	58, −15, 27
	Right	Superior temporal gyrus	4.23	60, −1, −8
	Right	Occipital cortex	5.32	42, −78, 7
NTSD > TSD	Left	Cerebellum (lobule VIIa)	3.39	−38, −59, −44

genu of the corpus callosum at a corrected $P \leq 0.016$. Increased FA was found in the cerebellum (lobule IX) (Fig. 2C, Table 3).

When comparing NTSD and TSD directly, TSD-specific differences in fiber tract integrity were found in the bilateral middle/inferior frontal gyrus, genu of the corpus callosum, and putamen, as well as in the right premotor cortex and anterior limb/genu of the internal capsule. The NTSD group demonstrated changes in the white matter underlying the bilateral middle cingulate gyrus, left primary sensorimotor cortex, and left inferior parietal lobule at a corrected $P \leq 0.016$ (Fig. 2D, Table 3).

No statistical differences were found between white matter abnormalities and disorder duration in either the TSD or the NTSD group.

Discussion

Our results are the first to describe differential brain abnormalities in two classes of adult-onset primary focal dystonia, TSD and NTSD, and thus address potential microstructural alterations underlying the task specificity in dystonia. A direct comparison between the TSD and NTSD groups indicated TSD-specific diffuse GMV changes in the brain regions controlling different levels of sensorimotor processing, such as the primary somatosensory, middle frontal, superior/inferior temporal gyri, middle/posterior cingulate cortex, occipital cortex, striatum, and cerebellum (lobules VI-VIIa). These GMV changes were accompanied by fiber tract aberrations in the genu of the corpus callosum and anterior limb/genu of the internal

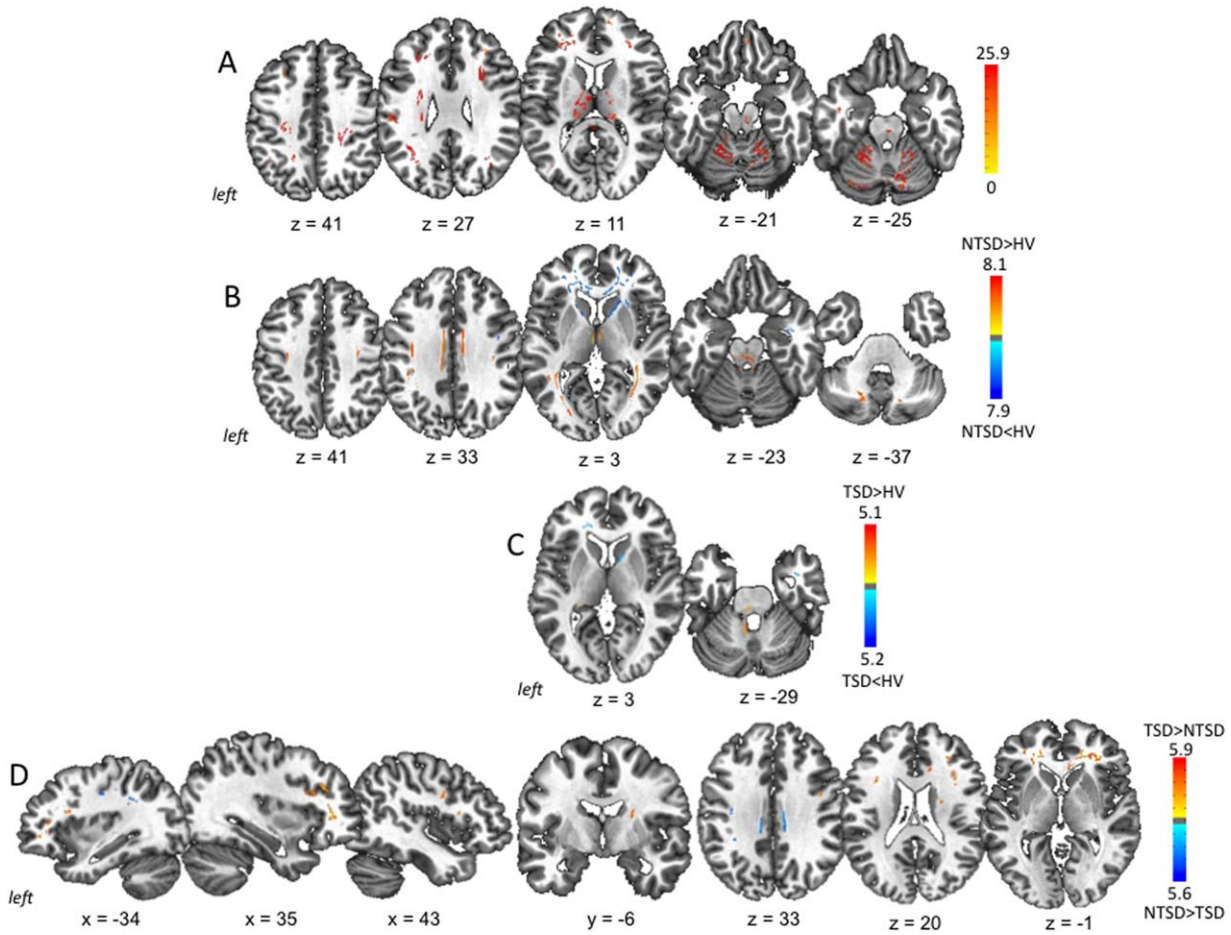

FIG. 2. White matter abnormalities in TSD and NTSD. (**A**) Initial analysis of variance (ANOVA) comparing fractional anisotropy (FA) as a measure of white matter integrity and coherence between TSD, NTSD, and healthy controls. (**B**) Abnormal FA in the NTSD group compared with healthy subjects. (**C**) Abnormal FA in the TSD group compared with healthy subjects. (**D**) Differences in FA between TSD and NTSD groups. Brain abnormalities are shown on a series of axial, sagittal, and coronal sections in the standard MNI space. The corresponding coordinates of peak changes are given in Table 2. The color bars represent *F* score (**A**) and *t* scores (**B, C, D**), respectively. TSD, task-specific dystonia; NTSD, non–task-specific dystonia.

capsule as well as the white matter changes underlying the premotor cortex, middle/inferior frontal, and inferior temporal gyri. Conversely, NTSD-specific GMV changes were limited to the left cerebellum (lobule VIIa) only, with fiber tract abnormalities underlying the primary sensorimotor, middle cingulate cortex and inferior parietal lobe. The presence of two distinct microstructural patterns in TSD and NTSD provides evidence that these two dystonia subclasses likely follow divergent pathophysiological mechanisms possibly precipitated by different triggers. These findings also point to multi-level, complex alterations of the sensorimotor integration and control for production of a highly learned task, such as writing or speaking.

Common Changes in TSD and NTSD

Compared with healthy controls, both TSD and NTSD groups showed similarly increased GMV in the primary sensorimotor cortex (albeit right in TSD and left in NTSD), which may relate to abnormalities of the motor control leading to involuntary muscle contractions. Another common feature shared by both focal dystonia classes was the involvement of the cerebellum, which gives further credence, from a structural perspective, to its role in dystonia pathophysiology.[22-24] Specifically, gray matter changes in the cerebellar lobules VI-VII were shared by both TSD and NTSD when compared with controls. Importantly, the anatomical/lobular location and laterality of these changes (bilateral in TSD and left in NTSD) was different between TSD and NTSD. Activation of the cerebellar cortex and dentate nucleus has been postulated to be important in consolidating learning.[25] In particular, efferent fibers from the lobules VI-VII project to the association cortices, such as prefrontal, parietal and superior temporal regions.[26] Because the cerebello-thalamo-cortical tract facilitates intracortical inhibition via the projections to interneurons in the sensorimotor cortices,[27] reduction in its fiber tract integrity

TABLE 3. White matter changes between task-specific dystonia (TSD), non–task-specific dystonia (NTSD) and controls

		Brain region	F-score	x,y,z
Initial ANOVA	Left	Middle frontal gyrus	15.65	−25, 34, 2
	Right	Middle frontal gyrus	15.04	34, 36, 1
	Left	Primary sensorimotor cortex	17.66	−24, −31, 47
	Right	Primary sensorimotor cortex	15.82	23, −32, 48
	Left	Occipital cortex	13.20	−34, −73, 3
	Right	Occipital cortex	11.39	34, −71, −7
	Left	Corpus callosum (genu)	23.51	−8, 29, 1
	Right	Corpus callosum (genu)	22.02	4, 26, 1
	Left	Corpus callosum (splenium)	23.30	−4, −33, 20
	Right	Corpus callosum (splenium)	25.22	1, −39, 13
	Left	Thalamus	17.24	−12, −6, 13
	Right	Thalamus	16.97	15, −15, 17
		Midbrain/pons	13.79	−4, −21, −8
	Left	Cerebellum (lobules VI/VIIa)	11.62	−17, −57, −24
	Right	Cerebellum (lobules VI/VIIa)	11.26	14, −49, −25
	Left	Operculum/insula	13.11	−27, −1, 28
	Left	Inferior parietal lobule/ supramarginal gyrus	12.97	−42, −47, 31
	Left	Middle temporal gyrus	17.91	−40, −44, −2
	Left	Inferior temporal gyrus	14.29	−43, −7, −25

White matter changes in NTSD/TSD vs. controls

			T-score	x,y,z
	Decreased fractional anisotropy			
NTSD vs. Controls	Left	Middle/inferior frontal gyri	−7.46	−31, 43, −2
	Right	Middle/inferior frontal gyri	−5.41	31, 42, −2
	Left	Corpus callosum (genu/body)	−7.95	−16, 36, 0
	Right	Corpus callosum (genu/body)	−7.24	13, 25, 18
	Left	Internal capsule (anterior limb/genu)	−4.21	−18, 16, 2
	Right	Internal capsule (anterior limb/genu)	−5.54	11, 5, −5
	Right	Primary sensorimotor cortex	−3.99	48, 2, 28
	Right	Inferior temporal gyrus	−5.69	44, 1, −32
	Increased fractional anisotropy			
		Corpus callosum (splenium)	4.82	0, −37, 17
	Left	Cingulate gyrus	7.38	−9, −8, 33
	Right	Cingulate gyrus	4.62	9, −9, 34
	Left	Occipital cortex	5.72	−24, −80, 4
	Right	Occipital cortex	6.40	37, −47, 1
		Midbrain/pons	3.99	−9, −28, −26
	Left	Cerebellum (lobule VIIa)	6.17	−21, −68, −39
	Right	Cerebellum (lobule VIIa)	6.07	15, −74, −36
	Right	Ventral thalamus	5.22	3, −13, 3
	Decreased fractional anisotropy			
TSD vs. Controls	Left	Middle frontal gyrus	−4.45	−27, 42, −3
	Right	Middle frontal gyrus	−3.04	33, 42, −2
	Right	Internal capsule (anterior limb/genu)	−4.30	10, 5, 1
	Left	Corpus callosum (genu)	−3.79	−15, 37, 1
	Increased fractional anisotropy			
	Left	Cerebellum	3.97	−9, −51, −30

White matter changes in TSD vs. NTSD

			T-score	x,y,z
TSD > NTSD	Left	Middle/inferior frontal gyrus	5.15	−15, 34, −6
	Right	Middle/inferior frontal gyrus	5.92	23, 37, −3
	Left	Corpus callosum (genu)	5.42	−6, 28, 5
	Right	Corpus callosum (genu)	5.37	13, 31, 8
	Left	Putamen	3.24	−22, −5, 15

(Continued)

TABLE 3. *Continued*

White matter changes in TSD vs. NTSD				
			T-score	*x,y,z*
	Right	Putamen	3.86	23, −6, 14
	Right	Premotor cortex	4.17	45, 0, 28
	Right	Internal capsule (anterior limb/genu)	3.91	23, −4, 16
NTSD > TSD	Left	Middle cingulate cortex	4.58	−10, −31, 32
	Right	Middle cingulate cortex	4.67	10, −28, 34
	Left	Primary sensorimotor cortex	4.38	−37, −14, 31
	Left	Inferior parietal lobule	4.27	−35, −43, 32

has been shown to correlate with cortical activation and hyperexcitability.[28,29] Neuronal plastic changes have also been associated with cerebellar input,[30] raising the possibility of a morphometric relationship between the cerebellum and sensorimotor cortex. Whether this circuit causes excessive neuronal plasticity or triggers the dystonic cascade is unknown, but the presence of microstructural changes provides further support to the possibility that the cerebello-thalamo-cortical system is involved in dystonia as an endophenotypic trait[31,32] and likely plays an important role in the generation of task-related behaviors.

The GMV decreases in the anterior dorsal putamen and ventral striatum were observed in NTSD but not TSD compared with controls possibly because of the variability in striatal volumes and topographic location of abnormalities among patients with writer's cramp and laryngeal dystonia, which may have induced a cancellation effect during the aggregate analysis. However, a direct comparison between NTSD and TSD clearly revealed the striatal differences between these groups in the anterior dorsal putamen and caudate nucleus as well as ventral striatum. Our findings are in line with the well-known predilection for striatal lesions to trigger dystonia[33,34] as well as previous reports of striatal GMV changes in all four focal dystonias investigated here.[6,7,10,11,14,15,35-37] An inverse correlation between symptom severity and putamen volume in cervical dystonia also has been described.[36] In considering this, we postulate that, from a microstructural aspect, the striato-pallido-thalamo-cortical network may differentially change based on the nature or extent of motor tasks. The order of evolution of these changes and their relationship to abnormal metabolic activity, aberrant cortical inhibition and hyperexcitabilty, or neuroplastic changes need to be investigated in future studies.

Distinct Changes in TSD and NTSD

In contrast to NTSD, the comparison between TSD and controls found wider-spread GMV abnormalities involving the left premotor cortex and operculum/insula. This may stem from the left hemispheric dominance of sensorimotor planning of speech and writing in right-handed individuals. In addition, a negative correlation between symptom duration and right premotor cortex GMV in TSD speaks to a cortical reorganization of the contralateral motor circuitry and possible "wearing off" of some aspects of motor planning as the disorder persists. Gray matter volume increases in the left inferior parietal cortex and right supramarginal and superior temporal gyri may have further impact on sensorimotor processing, such as integration of spatial orientation and attention to task-relevant cognitive, sensory and motor information.[38,39] The fiber tract abnormalities in the middle/inferior frontal gyri, premotor cortex, corpus callosum, and internal capsule in TSD appear to be tied to the broader cortical changes found in this group. Thus, the argument can be made that increased GMV in these regions may reflect a primary pathophysiological process specific to TSD.

The presence of increased GMV in the bilateral cerebellum and left thalamus as well as decreased GMV in the occipital cortex was specific to NTSD but not TSD when compared with controls. These changes have been previously described in morphometric studies involving separate blepharospasm and cervical dystonia patients.[11,16,35] However, the direct comparisons between NTSD and TSD showed GMV abnormalities in the left cerebellum only. Because all of the cortical changes in the NTSD group failed to segregate out in TSD versus NTSD comparisons, we suggest that limited cortical gray matter alterations may be a characteristic feature of NTSD attributable in part to a lesser requirement for higher sensorimotor and cognitive control for task production as in the case of TSD.

Conversely, diffuse changes of axonal coherence observed in NTSD, when compared with controls, highlight a more epigenetic origin causing direct or compensatory changes in the cortical, subcortical, and cerebellar fiber tracts. Paradoxically, the between-group comparisons indicated diffuse FA differences

specific to TSD compared with focal changes seen in NTSD, further reflecting possible underlying inherent differences in the nature of white matter abnormalities among these dystonia subclasses.

Limitations

The number of subjects with each dystonia form was relatively small. We previously showed that increasing the number of subjects resulted in a wider spread of GMV changes when pre-processing was held constant.[3] This was especially apparent in the cortical regions. However, because the primary aim of this study was to investigate the microstructural changes between TSD and NTSD, the composite *n* for each group was 24 and 23, respectively. Therefore, our results lacking significance is unlikely.

As it is the case with neuroimaging studies in general, our study did not allow for sorting out cause from consequence in the pathophysiology of TSD and NTSD, because these techniques are usually unable to directly differentiate between primary and secondary brain changes. However, our study is the first to examine the extent of brain differences between TSD and NTSD and by this adds valuable information for future investigation, such as targeted evaluation of postmortem tissue from these patients and cross-disciplinary studies to distinguish between the primary and secondary causes of this disorder.

In summary, the current study provides new insights into the structural brain changes in TSD and NTSD, because it reveals the existence of unique microstructural phenotypes for both classes. Future studies will need to elucidate the extent of relationships between these changes and divergent pathophysiological triggers in both TSD and NTSD. ■

Acknowledgments: We thank Winona Tse, MD, Catherine Cho, MD, and Ann Hunt, MD, for patient referral, and Frank Macaluso, Charles Adapoe, Heather Alexander, and Manjula Khubchandani, PhD, for help with data acquisition.

References

1. Zoons E, Booij J, Nederveen AJ, Dijk JM, Tijssen MA. Structural, functional and molecular imaging of the brain in primary focal dystonia: a review. Neuroimage 2011;56:1011-1020.
2. Neychev VK, Gross RE, Lehericy S, Hess EJ, Jinnah HA. The functional neuroanatomy of dystonia. Neurobiol Dis 2011;42:185-201.
3. Ramdhani RA, Simonyan K. Primary dystonia: conceptualizing the disorder through a structural brain imaging lens. Tremor and Hyperkinetic Movements 2013.
4. Garraux G, Bauer A, Hanakawa T, Wu T, Kansaku K, Hallett M. Changes in brain anatomy in focal hand dystonia. Ann Neurol 2004;55:736-739.
5. Delmaire C, Vidailhet M, Elbaz A, et al. Structural abnormalities in the cerebellum and sensorimotor circuit in writer's cramp. Neurology 2007;69:376-380.
6. Granert O, Peller M, Jabusch HC, Altenmuller E, Siebner HR. Sensorimotor skills and focal dystonia are linked to putaminal grey-matter volume in pianists. J Neurol Neurosurg Psychiatry 2011;82:1225-1231.
7. Egger K, Mueller J, Schocke M, et al. Voxel based morphometry reveals specific gray matter changes in primary dystonia. Mov Disord 2007;22:1538-1542.
8. Delmaire C, Vidailhet M, Wassermann D, et al. Diffusion abnormalities in the primary sensorimotor pathways in writer's cramp. Arch Neurol 2009;66:502-508.
9. Simonyan K, Tovar-Moll F, Ostuni J, et al. Focal white matter changes in spasmodic dysphonia: a combined diffusion tensor imaging and neuropathological study. Brain 2008;131(Pt 2):447-459.
10. Simonyan K, Ludlow CL. Abnormal structure-function relationship in spasmodic dysphonia. Cereb Cortex 2012;22:417-425.
11. Draganski B, Thun-Hohenstein C, Bogdahn U, Winkler J, May A. "Motor circuit" gray matter changes in idiopathic cervical dystonia. Neurology 2003;61:1228-1231.
12. Colosimo C, Pantano P, Calistri V, Totaro P, Fabbrini G, Berardelli A. Diffusion tensor imaging in primary cervical dystonia. J Neurol Neurosurg Psychiatry 2005;76:1591-1593.
13. Walsh RA, Whelan R, O'Dwyer J, et al. Striatal morphology correlates with sensory abnormalities in unaffected relatives of cervical dystonia patients. J Neurol 2009;256:1307-1313.
14. Black KJ, Ongur D, Perlmutter JS. Putamen volume in idiopathic focal dystonia. Neurology 1998;51:819-824.
15. Etgen T, Muhlau M, Gaser C, Sander D. Bilateral grey-matter increase in the putamen in primary blepharospasm. Journal of neurology, neurosurgery, and psychiatry 2006;77:1017-1020.
16. Horovitz SG, Ford A, Najee-Ullah MA, Ostuni JL, Hallett M. Anatomical correlates of blepharospasm. Translational Neurodegeneration 2012;1:12.
17. Ashburner J. A fast diffeomorphic image registration algorithm. NeuroImage 2007;38:95-113.
18. Forman SD, Cohen JD, Fitzgerald M, Eddy WF, Mintun MA, Noll DC. Improved assessment of significant activation in functional magnetic resonance imaging (fMRI): use of a cluster-size threshold. Magn Reson Med 1995;33:636-647.
19. Ward BD. Simultaneous inference for fMRI data. 2000.
20. Smith SM, Jenkinson M, Johansen-Berg H, et al. Tract-based spatial statistics: voxelwise analysis of multi-subject diffusion data. Neuroimage 2006;31:1487-1505.
21. Smith SM, Nichols TE. Threshold-free cluster enhancement: addressing problems of smoothing, threshold dependence and localisation in cluster inference. Neuroimage 2009;44:83-98.
22. Eidelberg D, Moeller JR, Antonini A, et al. Functional brain networks in DYT1 dystonia. Ann Neurol 1998;44:303-312.
23. Ceballos-Baumann AO, Sheean G, Passingham RE, Marsden CD, Brooks DJ. Botulinum toxin does not reverse the cortical dysfunction associated with writer's cramp: a PET study. Brain 1997;120:571-582.
24. Galardi G, Perani D, Grassi F, et al. Basal ganglia and thalamocortical hypermetabolism in patients with spasmodic torticollis. Acta Neurol Scand 1996;94:172-176.
25. Doyon J, Song AW, Karni A, Lalonde F, Adams MM, Ungerleider LG. Experience-dependent changes in cerebellar contributions to motor sequence learning. Proc Natl Acad Sci U S A 2002;99:1017-1022.
26. Kelly RM, Strick PL. Cerebellar loops with motor cortex and prefrontal cortex of a nonhuman primate. J Neurosci 2003;23:8432-8444.
27. Molinari M, Filippini V, Leggio MG. Neuronal plasticity of interrelated cerebellar and cortical networks. Neuroscience 2002;111:863-870.
28. Argyelan M, Carbon M, Niethammer M, et al. Cerebellothalamocortical connectivity regulates penetrance in dystonia. J Neurosci 2009;29:9740-9747.
29. Niethammer M, Carbon M, Argyelan M, Eidelberg D. Hereditary dystonia as a neurodevelopmental circuit disorder: Evidence from neuroimaging. Neurobiol Dis 2011;42:202-209.
30. Doyon J, Owen AM, Petrides M, Sziklas V, Evans AC. Functional anatomy of visuomotor skill learning in human subjects examined with positron emission tomography. Eur J Neurosci 1996;8:637-648.
31. Quartarone A, Pisani A. Abnormal plasticity in dystonia: Disruption of synaptic homeostasis. Neurobiol Dis 2011;42:162-170.
32. Quartarone A, Morgante F, Sant'angelo A, et al. Abnormal plasticity of sensorimotor circuits extends beyond the affected body part in focal dystonia. J Neurol Neurosurg Psychiatry 2008;79:985-990.

33. Marsden CD, Obeso JA, Zarranz JJ, Lang AE. The anatomical basis of symptomatic hemidystonia. Brain 1985;108:463-483.

34. Vitek JL. Pathophysiology of dystonia: a neuronal model. Mov Disord 2002;17(Suppl 3):S49-S62.

35. Obermann M, Yaldizli O, De Greiff A, et al. Morphometric changes of sensorimotor structures in focal dystonia. Mov Disord 2007;22:1117-1123.

36. Draganski B, Schneider SA, Fiorio M, et al. Genotype-phenotype interactions in primary dystonias revealed by differential changes in brain structure. NeuroImage 2009;47:1141-1147.

37. Pantano P, Totaro P, Fabbrini G, et al. A transverse and longitudinal MR imaging voxel-based morphometry study in patients with primary cervical dystonia. Am J Neuroradiol 2011;32:81-84.

38. Gottlieb J. From thought to action: the parietal cortex as a bridge between perception, action, and cognition. Neuron 2007; 53:9-16.

39. Gottlieb J, Balan P, Oristaglio J, Suzuki M. Parietal control of attentional guidance: the significance of sensory, motivational and motor factors. Neurobiology of Learning and Memory 2009;91: 121-128.